

Time dependence of susceptible-infected-susceptible epidemics on networks with nodal self-infections

Van Mieghem, Piet; Wang, Fenghua

DOI

[10.1103/PhysRevE.101.052310](https://doi.org/10.1103/PhysRevE.101.052310)

Publication date

2020

Document Version

Final published version

Published in

Physical Review E

Citation (APA)

Van Mieghem, P., & Wang, F. (2020). Time dependence of susceptible-infected-susceptible epidemics on networks with nodal self-infections. *Physical Review E*, 101(5), 1-10. Article 052310. <https://doi.org/10.1103/PhysRevE.101.052310>

Important note

To cite this publication, please use the final published version (if applicable). Please check the document version above.

Copyright

Other than for strictly personal use, it is not permitted to download, forward or distribute the text or part of it, without the consent of the author(s) and/or copyright holder(s), unless the work is under an open content license such as Creative Commons.

Takedown policy

Please contact us and provide details if you believe this document breaches copyrights. We will remove access to the work immediately and investigate your claim.

Time dependence of susceptible-infected-susceptible epidemics on networks with nodal self-infections

Piet Van Mieghem^{*} and Fenghua Wang

Delft University of Technology, Faculty of Electrical Engineering, Mathematics and Computer Science, P.O. Box 5031, 2600 GA Delft, The Netherlands



(Received 4 March 2020; accepted 28 April 2020; published 18 May 2020)

The average fraction of infected nodes, in short the prevalence, of the Markovian ε -SIS (susceptible-infected-susceptible) process with small self-infection rate $\varepsilon > 0$ exhibits, as a function of time, a typical “two-plateau” behavior, which was first discovered in the complete graph K_N . Although the complete graph is often dismissed as an unacceptably simplistic approximation, its analytic tractability allows to unravel deeper details, that are surprisingly also observed in other graphs as demonstrated by simulations. The time-dependent mean-field approximation for K_N performs only reasonably well for relatively large self-infection rates, but completely fails to mimic the typical Markovian ε -SIS process with small self-infection rates. While self-infections, particularly when their rate is small, are usually ignored, the interplay of nodal self-infection and spread over links may explain why absorbing processes are hardly observed in reality, even over long time intervals.

DOI: [10.1103/PhysRevE.101.052310](https://doi.org/10.1103/PhysRevE.101.052310)

I. INTRODUCTION

Inspired by the curious steady-state behavior of the Markovian ε -SIS (susceptible-infected-susceptible) process with arbitrarily small self-infection rate $\varepsilon > 0$, that was reported earlier in [1], we investigate the time dependence of the average fraction $y_N(\tau, \varepsilon^*; t)$ of infected nodes, briefly called the prevalence, in a graph with N nodes. Self-infections naturally occur in metapopulations, where each group consists of items (computers, animals, individuals, etc.) that are indistinguishable and exchangeable. Each group in a metapopulation can be represented by a node in the contact graph and interactions in that graph occur between groups, but also items within the group can infect other items in that same group. That intragroup type of infection is modeled as a self-infection. The ε -SIS epidemic process can also model information spread in social networks, where individuals themselves can generate information, which is then spread over links to neighbors. In social networks, happiness of persons [2] and obesity [3,4] has been modeled by an ε -SIS infection over a social contact network. Furthermore, the self-infection nodal process can also be interpreted as a “drift field” [5] that drives the infection in each node with a same strength. The infectious environment may be modeled by a self-infection process, usually with a small infection rate ε as a “background” or “imminent” infection [6]. The biological argument for such “background” infection stems from immunity of a species. When the virus dies out completely, the population will start losing immunity against that virus and a sudden reappearance of the virus may decimate a significant fraction of the population. Hence, the existence of very few infected nodes on average keeps the population fit against the virus because their immunity

system is constantly challenged. Related studies on contagion in networks consider a slightly more complex local rule than in ε -SIS, with either memory of infection doses [7] or a spontaneous self-infection dependent on a fixed number of infected neighbors [8].

Here, we focus on a simple, though stochastic, epidemic model with self-infections. In a graph G with N nodes, the viral state of a node i at time t is specified by a Bernoulli random variable $X_i(t) \in \{0, 1\}$: $X_i(t) = 0$ for a healthy node and $X_i(t) = 1$ for an infected node. Thus, at each time t , a node i can only be in one of the two states: *infected*, with probability $v_i(t) = \Pr[X_i(t) = 1] = E[X_i(t)]$ or *healthy*, with probability $1 - v_i(t)$, but susceptible to the virus. The curing process per node i is a Poisson process with rate δ and the infection rate per link is a Poisson process with rate β . Aside from infections over links from infected neighbors with rate β , the node i can also infect itself by a Poisson process with self-infection rate ε . Only when a node is infected, it can infect its direct, healthy neighbors. All Poisson processes are independent. This is the continuous-time description of the homogeneous self-infectious Markovian susceptible-infected-susceptible (ε -SIS) process on a contact graph. The ε -SIS model reduces to the “classical” SIS model when the self-infection rate is $\varepsilon = 0$. In the ε -SIS heterogeneous setting, the curing rate δ_i and self-infection rate ε_i are coupled to a node i and the infection rate β_{ij} specifies the link from node i to node j . In any continuous-time Markovian process, the interevent times are exponentially distributed [9, p. 210]. Thus, a self-infection rate ε means that, on average, every $1/\varepsilon$ time units a self-infection event occurs. Appendix analyzes the time-dependent ε -SIS Markovian process on the complete graph K_N and demonstrates that a closed form analytic solution is unlikely to exist.

Earlier, the ε -SIS model was introduced in [10] to compute a realistic steady state of the SIS epidemic on any finite graph

*P. F. A. VanMieghem@tudelft.nl

[11], close to the mean-field steady state, but very different from the steady state in the classical Markovian SIS process. The steady state of the Markovian SIS process (with $\varepsilon = 0$) on any finite graph is the absorbing state, that complicates the analysis [5,12] and, perhaps more importantly, is only attained after an exponentially in N long time [13,14]. Brightwell *et al.* [15] have shown that the (scaled) time to extinction or absorption *below* the mean-field epidemic threshold $\tau_c^{(1)} = \frac{1}{N}$ tends to a Gumbel distribution [9, p. 57] if $N \rightarrow \infty$. The mean-field SIS epidemic threshold in any graph is [16]

$$\tau_c^{(1)} = \frac{1}{\lambda_1},$$

where λ_1 is the largest eigenvalue of the adjacency matrix of the contact graph and lower bounds [17] the Markovian SIS epidemic threshold τ_c . In the ε -SIS model with $\varepsilon > 0$, there is no absorbing state and the Markov process is irreducible in a connected contact graph, which implies that there is a unique steady state, which is, for specially chosen self-infection rate ε as explained in [11], very close to observations and to the SIS mean-field steady state. We emphasize that the Markovian setting is important and that a mean-field analysis is unable to describe the “typical ε -SIS temporal behavior,” which is the topic of this paper.

II. TIME-DEPENDENT ε -SIS PREVALENCE IN THE COMPLETE GRAPH

A. Markovian setting

In [1], it was shown that there always exists a phase transition around τ_c^ε in the ε -SIS process on K_N , above which the effective infection rate $\tau = \frac{\beta}{\delta} > \tau_c^\varepsilon$ causes the average steady-state fraction $y_{\infty;N}(\tau, \varepsilon^*)$ of infected nodes, briefly called the prevalence, to approach the N -intertwined mean-field (NIMFA) prevalence [18]

$$y_{\infty;N}^{(1)}(\tau) = 1 - \frac{1}{(N-1)\tau}, \quad \tau > \frac{1}{N-1} = \tau_c^{(1)} \quad (1)$$

no matter how small, but not zero, the self-infection rate $\varepsilon^* = \frac{\varepsilon}{\delta}$ is. The phase transition τ_c^ε can be bounded by

$$\frac{1}{e} \left(\frac{10^{-s}}{\varepsilon^*(N-1)!} \right)^{\frac{1}{N-1}} < \tau_c^\varepsilon < \left(\frac{10^{-s}}{\varepsilon^*(N-1)!} \right)^{\frac{1}{N-1}},$$

where s specifies an agreed level for the onset of the phase transition at which $y_{\infty;N}(\tau, \varepsilon^*) = 10^{-s}$ is first reached, when τ is gradually increased from $\tau = 0$ at $y_{\infty;N}(0, \varepsilon^*) = \frac{\varepsilon^*}{1+\varepsilon^*}$ on.

The observation of a remarkable phase transition, increasingly explosive with the size N of the graph, was only possible by a purely analytical study the complete graph K_N (see Appendix in [1]). Unfortunately, that phase transition is hard to simulate for large N because the absorption time increases exponentially with N . Therefore, we present here simulations for small graphs of $N = 30$ nodes. The simulations were performed with our simulator, first described in [11] and later in [19, Appendix C]. The simulator has been tested in accuracy against exact solutions of the 2^N -Markovian SIS process [10] on small graphs of $N = 10$ nodes. The unit of time equals the average curing time, i.e., we have set in simulations the curing rate equal to $\delta = 1$ (so that $\varepsilon^* = \varepsilon$ here). For $N = 30$ in most

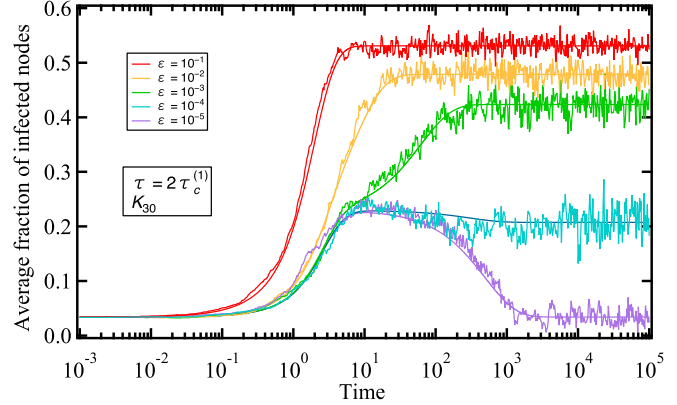


FIG. 1. The prevalence $y_N(\tau, \varepsilon^*; t)$ of the ε -SIS process on the complete graph K_N on $N = 30$ nodes with effective infection rate $\tau = 2\tau_c^{(1)} = \frac{2}{N-1}$ versus time on a logarithmic scale for various values of the self-infection rate ε . The epidemic started with one infected node. Both simulations and numerical solutions of the differential Eqs. (A7) and (A8) (smooth lines) are presented for each self-infection rate ε .

graphs, the absorbing time at which the virus is eradicated from the network is attained within 10^5 time units, i.e., within an interval equal to 10^5 times the average curing time.

We first concentrate on the complete graph, whose analysis is entirely possible analytically. Apart from simulations, averaged over 100 realizations, Fig. 1 also shows (in smooth lines) the prevalence $y_{30}(2\tau_c^{(1)}, \varepsilon^*; t)$ with $\tau_c^{(1)} = \frac{1}{29}$, obtained by numerically solving the set of differential equations of the ε -SIS process on the complete graph K_N in (A7) and (A8) of Appendix. The advantage of a small size N is that the entire time interval can be covered as illustrated in Fig. 1. Indeed, for small self-infection rates $\varepsilon = 10^{-5}$, the prevalence $y_{30}(2\tau_c^{(1)}, \varepsilon^*; t)$ in Fig. 1 starts with one infected node, increases rapidly, almost exponentially fast, toward about 20% of infected nodes between 1 and 10 time units, after which the prevalence $y_{30}(2\tau_c^{(1)}, \varepsilon^*; t)$ decreases slowly toward its steady state around 4%. Figure 1 generalizes the “classical”

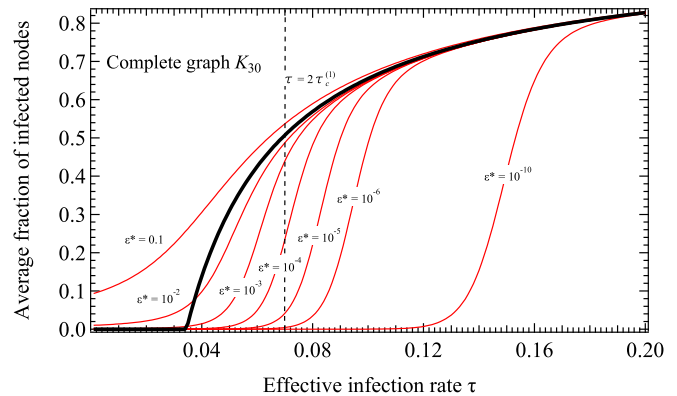


FIG. 2. The steady-state prevalence $y_{\infty;N}(\tau, \varepsilon^*)$ in a complete graph K_N on $N = 30$ nodes versus the effective infection rate τ , for various self-infection rates varying from $\varepsilon^* = 10^{-1}$ down to $\varepsilon^* = 10^{-10}$. The dotted line at $\tau = 2\tau_c^{(1)} = \frac{2}{N-1}$ corresponds to the setting in Fig. 1. The bold curve is the NIMFA steady-state prevalence (1).

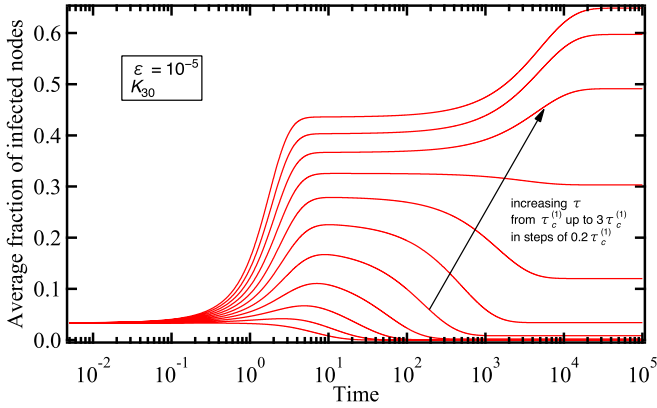


FIG. 3. The prevalence $y_N(\tau, \varepsilon^*; t)$ in the complete graph $N = 30$ versus time for self-infection rate $\varepsilon^* = 10^{-5}$ and effective infection rates $\tau_c^{(1)} \leq \tau \leq 3\tau_c^{(1)}$ and each curves differs $0.2\tau_c^{(1)}$ from its neighboring curves. The curves are numerical solution of the differential Eqs. (A7) and (A8).

$\varepsilon = 0$ SIS prevalence as a function of time, shown in [20, Fig. 12b] and [9, Fig. 17.2], where eventually the prevalence tends to zero for any effective infection rate τ in any graph with finite number N of nodes. When the self-infection rate ε is relatively high, the curves resemble the mean-field typical SIS behavior. In-between (for $\varepsilon = 10^{-3}$ and 10^{-4} in Fig. 1) characteristic ε -SIS behavior in time is exhibited, that we will explain below.

The disadvantage of a small size N , however, is that the transition from almost zero prevalence toward the NIMFA prevalence is not so steep as plotted in Fig. 2 for the steady-state prevalence, whose closed form

$$y_{\infty;N}(\tau, \varepsilon^*) = \frac{\sum_{k=1}^N \binom{N-1}{k-1} \tau^k \Gamma\left(\frac{\varepsilon^*}{\tau} + k\right)}{\sum_{k=0}^N \binom{N}{k} \tau^k \Gamma\left(\frac{\varepsilon^*}{\tau} + k\right)} \quad (2)$$

is derived in [1, Appendix]. Figure 2 compares the prevalence $y_{\infty;N}(\tau, \varepsilon^*)$ with the NIMFA $y_{\infty;N}^{(1)}(\tau)$ in (1), while a Markovian SIS process, in which dying out is prohibited [12] and thus absorption is prevented [21], is closer than NIMFA as shown in [21, Fig. 2] for the complete graph K_N . When N increases, the transition from small to NIMFA values is increasingly steep as illustrated in [1], resulting in a discontinuous step function if $N \rightarrow \infty$. However, in [1], only computations for the complete graph K_N were possible and, although it was claimed based upon physical arguments that the behavior is general for all graphs, that claim was not¹ supported by simulations. We fill this gap here and present simulations on various types of graphs. A key result is that the two plots in Figs. 1 and 2 are typical for any graph, as shown below, in the sense that the main behavior of the prevalence $y_N(\tau, \varepsilon^*; t)$ over time in any graph follows that in Fig. 1.

Figure 3 on the complete graph K_{30} with self-infection rate $\varepsilon^* = 10^{-5}$ shows the characteristic ε -SIS prevalence with two plateaus. For sufficiently high effective infection rates τ , the

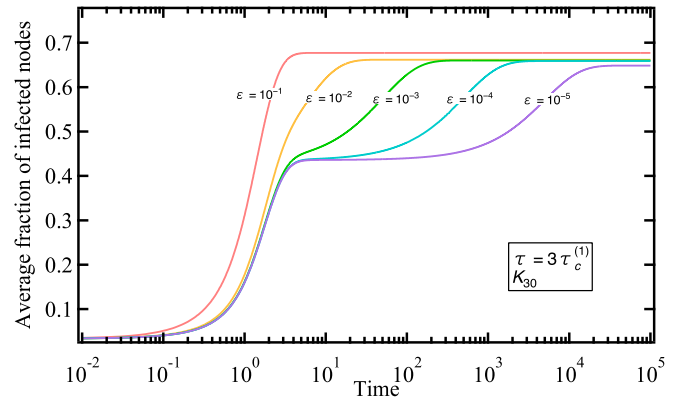


FIG. 4. The prevalence on K_{30} over time for a high effective infection rate $\tau = 3\tau_c^{(1)} = \frac{3}{29}$ and several self-infection rates ε . The curves are numerical solutions of the differential equations.

first plateau is rapidly reached and is due to link infections. The second, higher plateau is attained roughly around time $\frac{1}{\varepsilon}$ (in units of the average curing time). The interarrival time of self-infection events generated at each node is exponentially distributed with mean $\frac{1}{\varepsilon}$. The minimum of N -independent exponential random variables each with rate ε_i is again an exponential random variable with rate equal to their sum $\sum_{j=1}^N \varepsilon_j$, a property of the exponential distribution that lies at the basis of Markov theory.² Thus, the first appearance of self-infections is expected around time $\frac{1}{N\varepsilon}$, which is here about 3×10^3 time units. Figure 3 indeed illustrates that the onset toward the second plateau occurs around time 3×10^3 . The precise time changes as observed in Fig. 3 also depend on the effective infection rate τ over links because the onset starts for different τ , in particular for small τ , at slightly different times.

For smaller effective infection rates τ , the second plateau in the prevalence, that corresponds to its steady-state value, is lower than the first plateau caused by spreading over links in the graph. That lower value is due to a curious equilibrium between absorption (due to a series of rare curing events as explained in [1]) and self-infection. Recall that if $\varepsilon = 0$, thus in the “classical” Markovian SIS process without self-infections, the prevalence tends always to zero in any finite graph after sufficiently long time. In other words, the epidemics is eradicated from the graph with finite size N due a sequence of curing events that happens with very low, though positive, probability. Hence, the observation interval must be long enough to observe such a rare event of successive curing events, which explains the long absorption time in the classical $\varepsilon = 0$ stochastic SIS process. If the size N is larger,

²The Markov process is physically explained in [9, p. 399] for the shortest path problem with exponential link weights in a complete graph. Actually, that shortest path computation in the complete graph describes the exact SI Markovian process, leading to a shortest path tree that is a uniform recursive tree. Hence, for very small curing rates δ (and small self-infection rates that can be zero), equivalent to large effective infection rates τ , the viral spread in an ε -SIS in the complete graph follows a uniform recursive tree.

¹Alternatively, from (A11) by differentiating (A13) in the Appendix with respect to x , using (A5) and evaluating at $x = 1$ again leads to (2).

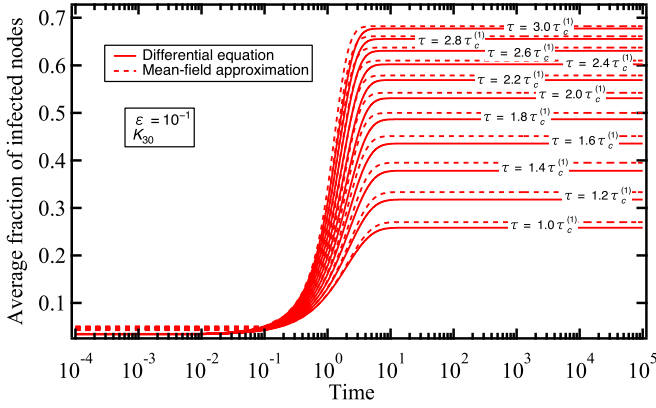


FIG. 5. The prevalence $y_N(\tau, \varepsilon^*; t)$ in the complete graph $N = 30$ versus time for self-infection rate $\varepsilon^* = 10^{-1}$ with the same values of effective infection rates τ as in Fig. 3. The mean-field approximation (6) (dotted lines) lies above ε -SIS Markovian prevalence, computed via the numerical solution of the differential Eqs. (A7) and (A8).

the steady state of the ε -SIS process in Fig. 2 sweeps fast, i.e., in a narrow range around τ_c^ε from virtually zero to the mean-field prevalence $y_{\infty;N}^{(1)}(\tau)$ in (1). That phenomenon for large N as reported in [1] is a kind of explosive percolation.

The onset of the second plateau, due to the self-infection process, is shown in Fig. 4 for several self-infection rates and a relatively high effective infection rate $\tau = 3\tau_c^{(1)} \approx 0.1$. On average, every $\frac{1}{\varepsilon}$ time units, a self-infection in each node is created, but the onset toward the second plateau is observed already earlier at about $\frac{1}{N\varepsilon}$ time units as explained above. Figure 2 illustrates that for higher effective infection rate τ and a fixed $\varepsilon^* \in [10^{-5}, 10^{-1}]$ band, the corresponding prevalence band decreases. In other words, for the same set of $\varepsilon^* = \varepsilon$ values as in Fig. 1 with $\tau = 2\tau_c^{(1)}$, the range of prevalence values in Fig. 4 with $\tau = 3\tau_c^{(1)}$ is considerably smaller. Furthermore, Fig. 2 at $\tau \approx 0.1$ illustrates that the curve $\varepsilon^* = 0.1$ slightly lies above the NIMFA bold curve (1), which explains why the corresponding curve Fig. 4 at large time slightly lies above the $\varepsilon^* = 10^{-2}$ to $\varepsilon^* = 10^{-4}$ curve and similarly why $\varepsilon^* = 10^{-5}$ lies below the NIMFA bold curve.

Figure 5 is the companion of Fig. 3 and demonstrates the ε -SIS process with high self-infection rate $\varepsilon = 0.1$. Both the link and the node spreading occur roughly at the same timescale and we observe a combined effect, leading to the “traditional mean-field” curves, specified by a tanh function [19] as computed in Sec. II B. In summary, only for small self-infection rate ε , anomalous behavior in the ε -SIS process with respect to the mean-field theory is observed.

B. N -intertwined mean-field approximation for ε -SIS

The governing differential equation of the N -intertwined mean-field approximation (NIMFA) for the heterogeneous ε -SIS epidemics on a graph with adjacency matrix A is

$$\frac{dv_i(t)}{dt} = -\delta_i v_i(t) + [1 - v_i(t)] \left(\sum_{j=1}^N a_{ij} \beta_{ij} v_j(t) + \varepsilon_i \right). \quad (3)$$

Indeed, the change with respect to time of the nodal infection probability $v_i(t)$ of node i at time t consists of two competing actors at time t : (a) if the node i is infected with probability $v_i(t)$, then node i can cure with own curing rate δ_i and (b) if the node i is healthy, a situation that occurs with probability $1 - v_i(t)$, then node i can be infected by all its infected neighbors [for which $a_{ij} = 1$ and infected with probability $v_j(t)$] at a specific link rate β_{ij} . In addition, the node i can infect itself with its own self-infection rate ε_i . The nodal differential Eq. (3) can be written as in [18,22] in matrix form

$$\frac{dv(t)}{dt} = \eta + Bv - \text{diag}(v)(Bv + c + \eta), \quad (4)$$

where the vector $v = (v_1, v_2, \dots, v_N)$, the self-infection vector $\eta = (\varepsilon_1, \varepsilon_2, \dots, \varepsilon_N)$, the curing vector $c = (\delta_1, \delta_2, \dots, \delta_N)$, and the $N \times N$ matrix B has elements $\beta_{ij} a_{ij}$. We denote the $N \times 1$ all one vector by u . The prevalence $y = \frac{u^T v}{N} = \frac{1}{N} \sum_{i=1}^N v_i(t)$, defined as the average fraction of infected nodes, follows as

$$N \frac{dy(t)}{dt} = u^T \eta - v^T (c + \eta) + (u - v)^T Bv. \quad (5)$$

The differential Eq. (4) can be transformed in various forms, analogously as in [9, Secs. 17.4–17.5]. Here, we confine to the complete graph K_N and to the homogeneous setting because the NIMFA differential equation can be solved analytically for K_N .

Only in the steady state, *symmetry* holds in regular graphs with degree r so that $v_{i\infty} = v_\infty = y_\infty$ and $v^T v = N y_\infty^2$ and the prevalence reduces to $y_\infty = 1 - \frac{1}{\tau r}$. Thus, only when the initial condition $v_i(0)$ is the same for each node i , symmetry applies and the mean-field prevalence in K_N equals $y_N^{(1)}(\tau, \varepsilon^*; t) = v(t) = v_i(t)$. After rewriting (3) in the normalized time $t^* = \delta t$,

$$\frac{dv(t)}{dt^*} = \varepsilon^* + \{\tau(N-1) - (1 + \varepsilon^*)\}v(t) - \tau(N-1)v^2(t),$$

we recognize a Riccati differential equation [23, Appendix C] with solution

$$\begin{aligned} y_N^{(1)}(\tau, \varepsilon^*; t) &= \frac{\tau(N-1) - (1 + \varepsilon^*)}{2\tau(N-1)} + \frac{\Upsilon}{2\tau(N-1)} \\ &\times \tanh \left[\frac{t}{2} \Upsilon + \text{arctanh} \left(\frac{\tau(N-1)(2y_0 - 1) + (1 + \varepsilon^*)}{\Upsilon} \right) \right], \end{aligned} \quad (6)$$

where

$$\Upsilon = \sqrt{[\tau(N-1) - (1 + \varepsilon^*)]^2 + 4\tau(N-1)\varepsilon^*}.$$

The mean-field approximation upper bounds the Markovian SIS process [17], which is manifested in Figs. 5 and 6.

III. BEYOND THE COMPLETE GRAPH

This section presents the time-dependent prevalence $y_N(\tau, \varepsilon^*; t)$ on other graphs than the complete graph K_N .

Figure 7 displays the characteristic ε -SIS prevalence $y_N(\tau, \varepsilon^*; t)$ and confirms that graphs, different than the com-

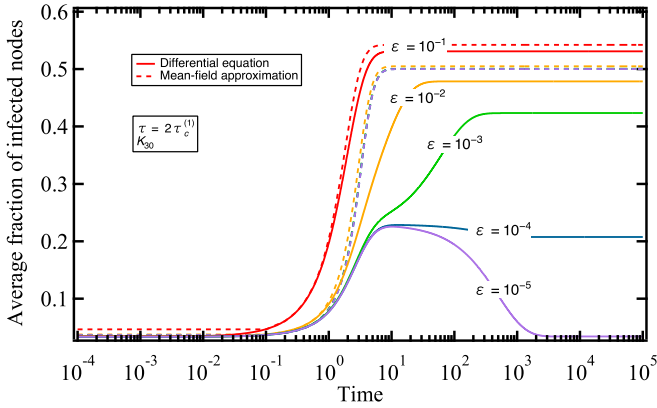


FIG. 6. The prevalence $y_N(\tau, \varepsilon^*; t)$ of the ε -SIS with same parameters as in Fig. 1 to which the mean-field approximation (6) is added. Same colors have same self-infection rate ε . In contrast to Fig. 5 for a large self-infection rate, the mean-field approximation (dotted line) deviates considerably for smaller self-infection rates.

plete graph K_N , essentially show the same characteristic ε -SIS prevalence time behavior, with two plateaus. A surprising fact concerns the Barabasi-Albert power law graph (BA) with $N = 500$ nodes. For large N and $\varepsilon = 0$, we would expect that the absorbing state is only reached after $O(e^{Nc})$ time units, where

the constant c depends upon the effective infection rate and the graph’s topology. However, the green curve for the BA graph, corresponding to $\tau = \frac{2.6}{\lambda_1}$, initially increases confirming that the effective infection rate lies above the epidemic threshold, but decreases relatively fast.

Figure 8 for an Erdős-Rényi (ER) graph with $N = 100$ nodes, on the other side, does not depict such decrease; the green curve stays much longer in the quasistationary state, as expected for an exponentially increasing absorbing time.

Figure 9 for the star graph (a center node with $N - 1$ leaves) is the companion of Fig. 3 for the complete graph. Both plots look amazingly similar. For the star graph with spectral radius $\lambda_1 = \sqrt{N - 1}$ and mean-field epidemic threshold $\tau_c^{(1)} = \frac{1}{\lambda_1} = \frac{1}{\sqrt{N - 1}}$, analytic computations [12] indicate that the actual epidemic threshold for sufficiently large N is $\tau_c = \frac{\alpha}{\sqrt{N - 1}}$ with $\alpha = \sqrt{\frac{\log N}{2}} + \frac{3}{2} \log \log N$. Although $N = 30$ is small, that estimate gives $\tau_c \simeq \frac{1.872}{\sqrt{29}}$, which explains that the lowest curve corresponding to $\tau = 2\tau_c^{(1)}$ just exceeds the (actual) epidemic threshold τ_c . Again, the “two plateaus” expose a clear manifestation of the Markovian ε -SIS time-dependent process and illustrate that the steady state of the average fraction of infected nodes can be understood from the complete graph computations: In contrast to the “classical” SIS process ($\varepsilon = 0$) where all prevalence curves eventually

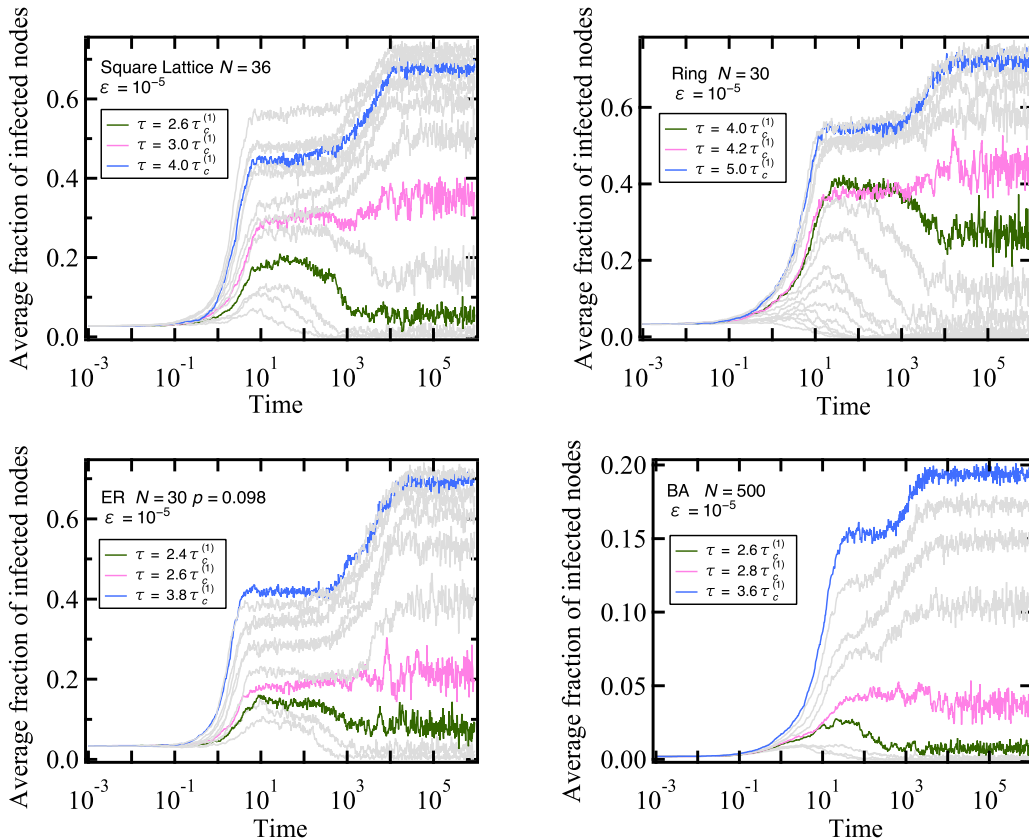


FIG. 7. The prevalence $y_N(\tau, \varepsilon^*; t)$ with self-infection rate $\varepsilon^* = 10^{-5}$ versus time for four different types of graphs: the square lattice with $N = 36$, the ring graph with $N = 30$, the Erdős-Rényi random graph with $N = 30$ and link density $p = 0.098$ and the Barabasi-Albert power law graph with $N = 500$. Initially, one node is infected and the plots are based upon (i.e., averaged over) 100 realizations of each ε -SIS process. The prevalence curves shown increase with a step of $\tau = 0.2\tau_c^{(1)}$. The three curves in color illustrate the three different behaviors: blue shows two plateaus and upward bending, red the almost constant plateau, and green depicts the downward bending.

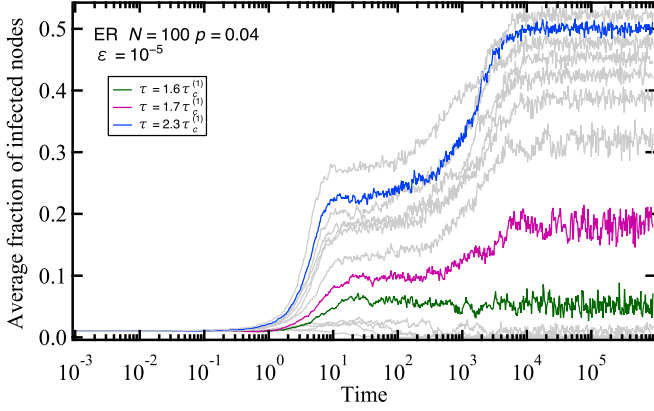


FIG. 8. The “two-plateau” ε -SIS prevalence curve versus time for an Erdős-Rényi (ER) graph with $N = 100$ nodes and link density $p = 2p_c$ and $\varepsilon = 10^{-5}$. The downward bending of the green curve only occurs for considerably larger times.

end up at zero (absorbing state), Fig. 9 and also Fig. 7 indicate that, in the steady state (not the metastable or quasistationary state!), all possible values of the prevalence between zero and the mean-field steady state are possible as claimed earlier in [1].

IV. CONCLUSION

The prevalence $y_N(\tau, \varepsilon^*; t)$ of the Markovian ε -SIS process with small self-infection rate $\varepsilon > 0$ has been studied as a function of time. The typical “two-plateau” behavior, first explained for the complete graph K_N based on analytic computations, is demonstrated to hold generally for other graphs than K_N as well. In fact, we claim that it may hold for any finite graph. In practice, if a disease or the spread of items on a graph can be modeled as a Markovian ε -SIS process with small self-infection rate ε , the second plateau may play a significant role: after the epidemics arrives at the first plateau (in relatively short time), the epidemics will

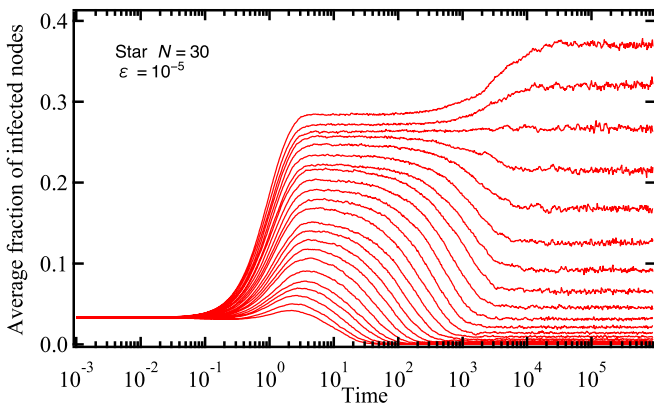


FIG. 9. The ε -SIS prevalence $y_N(\tau, \varepsilon^*; t)$ in the star graph on $N = 30$ node as a function of time (in units of the average curing time). Initially, one (leave) node is infected and the prevalence is averaged over 10^4 realizations. The curves depicted have an effective infection rate, starting with the lowest curve at $\tau = 2\tau_c^{(1)} = \frac{2}{\sqrt{N-1}}$ up to the highest curve $\tau = 6.4\tau_c^{(1)}$ with a step of $\tau = 0.2\tau_c^{(1)}$.

not disappear as in the “classical” $\varepsilon = 0$ SIS case nor stay constant as in the mean-field approximation, but will tend to the second plateau, that can be either higher or lower than the first plateau, depending on its self-infection rate ε .

The time-dependent mean-field approximation for K_N performs only reasonably well for relatively large self-infection rates, but completely fails to mimic the typical Markovian ε -SIS process with small self-infection rates. While self-infections, in particular when their rate is small, are usually ignored, we have shown that the interplay of nodal self-infection and spread over links may explain why absorbing processes are less observed in reality.

ACKNOWLEDGMENT

We are very grateful to Z. He and M. Achterberg for their inspiring discussions.

APPENDIX: DIFFERENTIAL EQUATION FOR THE MARKOVIAN ε -SIS PROCESS ON K_N

In spite of the simplicity of the Markovian continuous-time SIS model, there does not seem to exist an exact time-dependent solution for any graph. Most analytic results are known for the complete graph as shown in [9, Sec. 17.6]. Before elaborating on the exact analytic solution of the Markovian continuous-time SIS model on the complete graph K_N containing N nodes, we briefly review the classical mean-field approximation.

For the complete graph K_N , mean-field approximations are accurate [12,17]. Very likely, although there does not seem to be a rigorous proof, among all graphs, mean-field approximations are the most accurate in the complete graph. In the N -intertwined mean-field approximation (NIMFA) [18,22], the governing equation for the probability $v(t)$ of infection in a node at time t in a regular graph G with degree r equals

$$\frac{dv(t)}{dt} = r\beta(t)v(t)[1 - v(t)] - \delta(t)v(t), \quad (\text{A1})$$

where the infection rate $\beta(t)$ and the curing rate $\delta(t)$ are general non-negative real functions of time t . Since the rates are time varying, the infection and curing process are independent, inhomogeneous Poisson processes [9]. The differential Eq. (A1) can be solved exactly [24], resulting in

$$v(t) = \frac{\exp\left(\int_0^t [r\beta(u) - \delta(u)]du\right)}{\frac{1}{v_0} + r \int_0^t \beta(s) \exp\left(\int_0^s [r\beta(u) - \delta(u)]du\right)ds}, \quad (\text{A2})$$

where v_0 is the initial fraction of infected nodes. The ε -SIS companion of (A1) with time-dependent rates in a regular graph with degree r , assuming the same initial condition $v(0)$ in each node, is

$$\frac{dv(t)}{dt} = \varepsilon(t) + \{r\beta(t) - [\delta(t) + \varepsilon(t)]\}v(t) - r\beta(t)v^2(t). \quad (\text{A3})$$

Unfortunately, we could not solve (A3) explicitly as in (A2) mainly due to the first term $\varepsilon(t)$ at the right-hand side, which causes deviations from the Bernoulli differential equation.

As shown in [11] for regular graphs, the governing differential equations are precisely the same for NIMFA and the heterogeneous mean-field (HMF) approximation [25] of

Pastor-Satorras and Vespignani. Hence, Eq. (A1) constitutes a general SIS mean-field approximation for regular graphs. An interesting feature of (A1) is its independence on the size of the network, which avoids (or ignores) finite-size effects that often complicate studies of phase transitions. For regular graphs, the NIMFA average fraction of infected nodes $y(t) = v(t)$ and $y(t)$ is coined the order parameter in statistical physics. Equation (A1) with constant rates, $\beta(t) = \beta$ and $\delta(t) = \delta$, has been investigated earlier by Kephart and White [26]. Many variations on and extensions of the epidemic Kephart and White model have been proposed (see, e.g., [22,27,28]). In fact, the differential Eq. (A1) with constant rates has already appeared in earlier work before Kephart and White (see, e.g., [29,30]) and is also known as the logistic differential equation of population growth, first introduced by Verhulst [31].

1. Number of infected nodes in K_N

We consider the time-dependent ε -SIS process on the complete graph, where a positive self-infection rate ε is crucial for the existence of a nontrivial steady state as shown in [9, Chap. 17]. The number of infected nodes $M(t)$ at time t in the complete graph K_N is described by a continuous-time Markov process on $\{0, 1, \dots, N\}$ with the following rates:

$$M \mapsto M + 1 \text{ at rate } (\beta M + \varepsilon)(N - M),$$

$$M \mapsto M - 1 \text{ at rate } \delta M.$$

Every infected node heals with rate δ , which explains the transition rate $M \mapsto M - 1$. Every healthy node (of which there are $N - M$ at state M) has exactly M infected neighbors, each actively transferring the virus with rate β in addition to the self-infection rate ε . Alternatively, each of the M infected nodes can infect its $N - M$ healthy neighbors with a rate β and the $N - M$ healthy nodes can infect themselves with self-infection rate ε .

This Markov process $M(t)$ is a birth and death process with birth rate $\lambda_k = (\beta k + \varepsilon)(N - k)$ and death rate $\mu_k = k\delta$ when it is in a state with $M(t) = k$ infected nodes. The steady-state probabilities π_0, \dots, π_N , where $\pi_k = \lim_{t \rightarrow \infty} \Pr[M(t) = k]$, of a general birth-death process can be computed exactly [9, p. 230], [10] as

$$\pi_k = \pi_0 \binom{N}{k} \varepsilon^* \tau^{k-1} \frac{\Gamma(\frac{\varepsilon^*}{\tau} + k)}{\Gamma(\frac{\varepsilon^*}{\tau} + 1)} \quad (k > 0) \quad (\text{A4})$$

and

$$\pi_0 = \frac{1}{\sum_{k=0}^N \binom{N}{k} \tau^k \frac{\Gamma(\frac{\varepsilon^*}{\tau} + k)}{\Gamma(\frac{\varepsilon^*}{\tau})}}, \quad (\text{A5})$$

where the effective infection rate $\tau = \frac{\beta}{\delta}$ and $\varepsilon^* = \frac{\varepsilon}{\delta}$. Thus, π_0 is the steady-state probability that the complete graph K_N is infection free or overall healthy. When $\varepsilon \rightarrow 0$ for N fixed, we observe from (A4) that $\lim_{\varepsilon \rightarrow 0} \pi_k = 0$ for $k > 0$ and, consequently, that $\lim_{\varepsilon \rightarrow 0} \pi_0 = 1$, which reflects that the steady state of the SIS process (in any finite graph) is the overall-healthy state or absorbing state.

2. A generating function approach

We denote the probability that the number of infected nodes $M(t)$ at time t equals k (or that the ε -SIS process at time t is in state k) by

$$s_k(t) = \Pr[M(t) = k]. \quad (\text{A6})$$

By convention, we agree that $s_k(t) = 0$ if $k > N$ or if $k < 0$. Thus, $s_0(t)$ is the probability that the epidemic dies out at time t or that the complete graph K_N is infection free at time t , but only remains infection free provided the self-infection rate $\varepsilon = 0$. Further, the steady-state probabilities

$$\pi_k = \lim_{t \rightarrow \infty} s_k(t)$$

are explicitly known in (A4). The birth rate $\lambda_k = (\beta k + \varepsilon)(N - k) = -\beta k^2 + (N\beta - \varepsilon)k + N\varepsilon$ is quadratic in k and the death rate $\mu_k = \delta k$ is linear in k for any state $k \in \{0, 1, 2, \dots, N\}$. The time-dependent evolution of the constant birth and death process [9, p. 239] as well as the linear birth and death process is described in [9, p. 243]. Here, we study the quadratic birth and death process, whose solution has, by the best of our efforts, not yet appeared in the literature.

Applying the differential equations of a general birth and death process to ε -SIS process yields the set

$$s'_0(t) = \delta s_1(t) - N\varepsilon s_0(t), \quad (\text{A7})$$

$$s'_k(t) = \{\beta k^2 - (N\beta + \delta - \varepsilon)k - N\varepsilon\}s_k(t) + \{-\beta(k - 1)^2 + (N\beta - \varepsilon)(k - 1) + N\varepsilon\} \times s_{k-1}(t) + \delta(k + 1)s_{k+1}(t), \quad (\text{A8})$$

where all involved rates β , δ , and ε can depend upon time t . The first differential Eq. (A7) is incorporated in the general one (A8) for $k = 0$ since $s_{-1}(t) = 0$ by our convention. If $k = N$, then $\lambda_N = 0$ as well as $s_{N+1}(t) = 0$, so that (A8) reduces to

$$s'_N(t) = -\delta N s_N(t) + \{\beta(N - 1) + \varepsilon\}s_{N-1}(t).$$

The ε -SIS epidemic must always be in one of the possible states, which translates to $\sum_{k=0}^N s_k(t) = 1$.

Following the general method illustrated in [9, Secs. 11.3.3–11.3.4] for the constant and linear rate birth and death process, we start by defining the probability generating function (pgf)

$$\varphi(x, t) = E[x^{M(t)}] = \sum_{k=0}^N s_k(t)x^k \quad (\text{A9})$$

which we can equally well write as $\varphi(x, t) = \sum_{k=0}^{\infty} s_k(t)x^k$, according to the convention that $s_k(t) = 0$ if $k > N$ or if $k < 0$. For any probability generating function $\varphi_X(z) = E[z^X] = \sum_{k=0}^{\infty} \Pr[X = k]z^k$, the radius R of convergence around $z = 0$ in the complex z plane is at least equal to one, because for $|z| \leq 1$, it holds that $|\varphi_X(z)| \leq \sum_{k=0}^{\infty} \Pr[X = k]|z|^k \leq \sum_{k=0}^{\infty} \Pr[X = k] = \varphi_X(1) = 1$.

Theorem 1. In the time-dependent ε -SIS process on the complete graph K_N , the probability generating function $\varphi(x, t)$ of the number of infected nodes $M(t)$ at time t obeys the

partial differential equation

$$\frac{\partial \varphi}{\partial t} = (x-1) \left\{ -\beta x^2 \frac{\partial^2 \varphi}{\partial x^2} + [(N-1)\beta - \varepsilon]x - \delta \right\} \frac{\partial \varphi}{\partial x} + N\varepsilon \varphi. \tag{A10}$$

Proof. After multiplying both sides in (A8) by x^k and summing over all $k \geq 0$, the first line in (A8) is transformed as

$$T_1 = \sum_{k=0}^N \{ \beta k^2 - (N\beta + \delta - \varepsilon)k - N\varepsilon \} s_k(t) x^k.$$

With $\frac{\partial \varphi}{\partial x} = \sum_{k=0}^N k s_k(t) x^{k-1}$ and $\frac{\partial^2 \varphi}{\partial x^2} = \sum_{k=0}^N k(k-1) s_k(t) x^{k-2}$, we have

$$T_1 = \beta x^2 \frac{\partial^2 \varphi}{\partial x^2} - [(N-1)\beta + \delta - \varepsilon]x \frac{\partial \varphi}{\partial x} - N\varepsilon \varphi.$$

Similarly, the transform of the second line in (A8) taking our convention $s_{-1}(t) = 0$ into account is

$$T_2 = \sum_{k=1}^N \{ -\beta(k-1)^2 + (N\beta - \varepsilon)(k-1) + N\varepsilon \} s_{k-1}(t) x^k$$

leading to

$$T_2 = -\beta x^3 \frac{\partial^2 \varphi}{\partial x^2} + [(N-1)\beta - \varepsilon]x^2 \frac{\partial \varphi}{\partial x} + N\varepsilon x \varphi.$$

Finally, the transform of the third and last line in (A8) is, with $s_{N+1}(t) = 0$,

$$\begin{aligned} T_3 &= \delta \sum_{k=0}^N (k+1) s_{k+1}(t) x^k = \delta \sum_{k=1}^{N+1} k s_k(t) x^{k-1} \\ &= \delta \sum_{k=1}^N k s_k(t) x^{k-1} = \delta \frac{\partial \varphi}{\partial x}. \end{aligned}$$

Equating the three right-hand side contributions $T_1 + T_2 + T_3$ and the transform of the left-hand side in (A8) yields

$$\begin{aligned} \frac{\partial \varphi}{\partial t} &= -\beta x^2 (x-1) \frac{\partial^2 \varphi}{\partial x^2} + \{ (N-1)\beta x(x-1) - \varepsilon x(x-1) \\ &\quad - \delta(x-1) \} \frac{\partial \varphi}{\partial x} + N\varepsilon(x-1)\varphi. \end{aligned}$$

Thus, we find the partial differential Eq. (A10). ■

The factor $(x-1)$ at the right-hand side of (A10) is a consequence of the conservation of probability at any time t , namely, that $\varphi(1, t) = \sum_{k=0}^{\infty} s_k(t) = 1$, implying that the ε -SIS stochastic process is surely in one of the possible states. Furthermore, $\frac{\partial \varphi}{\partial x} \Big|_{x=1} = \sum_{k=0}^{\infty} k s_k(t)$ is the average number of infected nodes at time t . Hence, the average fraction of infected nodes at time t equals

$$y_N(\tau, \varepsilon; t) = \frac{1}{N} \frac{\partial \varphi(x, t)}{\partial x} \Big|_{x=1}. \tag{A11}$$

Initial condition. The ε -SIS process can start with a certain probability distribution, which then requires that the initial state vector $s(0) = (s_0(0), s_1(0), \dots, s_N(0))$ is given. When

precisely m nodes in K_N are infected initially at $t = 0$, then the boundary condition $\varphi(x, 0) = \sum_{k=0}^{\infty} \delta_{km} x^k = x^m$. Clearly, the value of $m > 0$ must exceed zero because $\varphi(0, t) = s_0(t)$ is the probability that the complete graph is infection free at time t and, in the long run, $\lim_{t \rightarrow \infty} \varphi(0, t) = \pi_0$ is given by (A5).

Confinement. In the sequel, we limit ourselves to constant rates: none of the infection rate β , self-infection rate ε , or curing rate δ are a function of time t . In addition, we assume that the ε -SIS process starts at $t = 0$.

Steady-state probability generating function $\varphi_{\infty}(x)$

The steady-state probability generating function (assuming constant rates) equals with (A4)

$$\begin{aligned} \lim_{t \rightarrow \infty} \varphi(x, t) &= \sum_{k=0}^{\infty} \lim_{t \rightarrow \infty} \Pr [M(t) = k] x^k \\ &= \sum_{k=0}^{\infty} \pi_k x^k = \varphi_{\infty}(x), \end{aligned}$$

where

$$\varphi_{\infty}(x) = \pi_0 + \frac{\varepsilon^* \pi_0}{\tau \Gamma\left(\frac{\varepsilon^*}{\tau} + 1\right)} \sum_{k=1}^N \binom{N}{k} \Gamma\left(\frac{\varepsilon^*}{\tau} + k\right) (\tau x)^k. \tag{A12}$$

Thus, if $\varepsilon = 0$, then $\pi_0 = 1$ and there holds that $\lim_{t \rightarrow \infty} \varphi(x, t) = \varphi_{\infty}(x) = 1$. If $\varepsilon > 0$, the steady-state probability generating function $\varphi_{\infty}(x)$ is a polynomial of degree N in x , which is more elegantly written as

$$\varphi_{\infty}(x) = \frac{\pi_0}{\Gamma\left(\frac{\varepsilon^*}{\tau}\right)} \sum_{k=0}^N \binom{N}{k} \Gamma\left(\frac{\varepsilon^*}{\tau} + k\right) (\tau x)^k \tag{A13}$$

and the general relation for any pgf, $\varphi_{\infty}(1) = 1$, also follows from (A5). Finally, $\varphi_{\infty}(x)$ is a function of three parameters

$$\varphi_{\infty}(x) = \varphi_{\infty}(x; \tau, \varepsilon^*, N).$$

The partial differential Eq. (A10) simplifies, in the steady state for $t \rightarrow \infty$ and $\frac{\partial \varphi}{\partial t} = 0$, to

$$-\beta x^2 \frac{\partial^2 \varphi_{\infty}}{\partial x^2} + \{ [(N-1)\beta - \varepsilon]x - \delta \} \frac{\partial \varphi_{\infty}}{\partial x} + N\varepsilon \varphi_{\infty} = 0. \tag{A14}$$

Introducing the integral for the gamma function $\Gamma(s) = \int_0^{\infty} u^{s-1} e^{-u} du$, valid for $\text{Re}(s) > 0$, into (A13) and invoking Newton's binomial leads to an integral representation³ of the

³ Assuming a positive real x and letting $w = (\tau x)u$, we find

$$\varphi_{\infty}(x) = \frac{\pi_0}{(\tau x)^{\frac{\varepsilon^*}{\tau}} \Gamma\left(\frac{\varepsilon^*}{\tau}\right)} \int_0^{\infty} e^{-\frac{w}{\tau x}} w^{\frac{\varepsilon^*}{\tau}-1} (1+w)^N dw.$$

We conclude that the steady-state probability generating function $\varphi_{\infty}(x)$ can be written as

$$\varphi_{\infty}(x) = \frac{\pi_0}{(\tau x)^{\frac{\varepsilon^*}{\tau}}} U\left(\frac{\varepsilon^*}{\tau}, \frac{\varepsilon^*}{\tau} + 1 + N, \frac{1}{\tau x}\right), \tag{A15}$$

steady-state probability generating function for $\varepsilon > 0$:

$$\varphi_\infty(x; \tau, \varepsilon^*, N) = \frac{\pi_0}{\Gamma\left(\frac{\varepsilon^*}{\tau}\right)} \int_0^\infty u^{\frac{\varepsilon^*}{\tau}-1} e^{-u} (1 + \tau u x)^N du. \tag{A16}$$

3. General solution of the partial differential Eq. (A10)

Theorem 2. In the time-dependent ε -SIS process on the complete graph K_N with constant infection rate β , self-infection rate ε , and curing rate δ , the probability generating function $\varphi(x, t)$ of the number of infected nodes $M(t)$ at time t can be written as a Laplace transform

$$\varphi(x, t) = \int_0^\infty e^{-ct} g(x; c) dc, \tag{A17}$$

where the function $g(x, c)$ obeys the differential equation

$$\begin{aligned} & -x^2(x-1) \frac{d^2 g}{dx^2} + \left\{ \left[(N-1) - \frac{\varepsilon^*}{\tau} \right] x - \frac{1}{\tau} \right\} (x-1) \frac{dg}{dx} \\ & + \frac{1}{\tau} [N\varepsilon^*(x-1) + c^*] g = 0 \end{aligned} \tag{A18}$$

and $\tau = \frac{\beta}{\delta}$, $\varepsilon^* = \frac{\varepsilon}{\delta}$, and $c^* = \frac{c}{\delta} \geq 0$.

Proof. The usual recipe of the separation of the variables t and x , by assuming that a solution in product form as $\varphi(x, t) = g(x)h(t)$ exists, transforms (A10) to

$$\begin{aligned} \frac{\partial \ln h}{\partial t} = \frac{(x-1)}{g} \left\{ -\beta x^2 \frac{d^2 g}{dx^2} + \left[(N-1)\beta - \varepsilon \right] x - \delta \right\} \frac{dg}{dx} \\ + N\varepsilon g \end{aligned} \tag{A19}$$

By taking the derivative of both sides with respect to x , we find with $\frac{\partial}{\partial x} \frac{\partial \ln h}{\partial t} = 0$ that

$$\frac{(x-1)}{g} \left\{ -\beta x^2 \frac{d^2 g}{dx^2} + \left[(N-1)\beta - \varepsilon \right] x - \delta \right\} \frac{dg}{dx} + N\varepsilon g = c_1, \tag{A20}$$

where c_1 is a constant that is neither a function of x nor of t because the left-hand side in (A20) is independent of t . Similarly, by taking the derivative of both sides in (A19) with respect to t , we find that

$$\frac{\partial \ln h}{\partial t} = c_2 \tag{A21}$$

and (A19) shows that $c_1 = c_2 = -c$. We rewrite (A20) with $\varepsilon^* = \frac{\varepsilon}{\delta}$ and $c^* = \frac{c}{\delta}$ to find (A18).

From (A21), we find $h(t) = h(0)e^{-ct}$ for the time $t \geq 0$. If c were complex and $\text{Im}(c) \neq 0$, then $h(t) = h(0)e^{-\text{Re}(c)t} [\cos t \text{Im}(c) + i \sin t \text{Im}(c)]$ and $\varphi(x, t) = g(x)h(t)$ is generally complex for $t > 0$. However, the definition (A9) of the pgf $\varphi(x, t)$ illustrates that

where the confluent hypergeometric function [32, Chap. 13.2.8]

$$U(a, b, z) = \frac{1}{\Gamma(a)} \int_0^\infty e^{-z} w^{a-1} (1+w)^{b-a-1} dw$$

is one of the independent solutions of Kummer’s differential equation $x \frac{d^2 f}{dx^2} + (b-x) \frac{df}{dx} - af = 0$ (see, e.g., [32, Chap. 13]).

$\varphi(x, t)$ is real for real x at any time $t \geq 0$. Hence, c must be real. Moreover, since the asymptotic pgf $\lim_{t \rightarrow \infty} \varphi(x, t) = \varphi_\infty(x)$ exists, c must be non-negative, otherwise $\lim_{t \rightarrow \infty} h(t) = h(0) \lim_{t \rightarrow \infty} e^{-ct} = \infty$. We conclude that the eigenvalue c is real and non-negative.

The general solution of the eigenvalue differential Eq. in c consists of a linear combination $\sum_{c \geq 0} e^{-ct} g(x; c)$ if the eigenvalues c are discrete. Generally, one readily verifies that $\varphi(x, t) = \int_0^\infty e^{-ct} g(x; c) dc$ satisfies the partial differential Eq. (A10) provided that $g(x; c)$ is a solution of the differential Eq. (A18) as a function of the “eigenvalue” c . ■

In fact, we need to solve an eigenvalue problem that can be expanded in a Sturm-Liouville series [33]. For $c = 0$, the differential Eq. (A18) reduces to the differential (A14) and we conclude that

$$g(x, 0) = \varphi_\infty(x).$$

The ε -SIS process on the complete graph K_N with N nodes is described by a general birth-death process by the differential equations (A7) and (A8). This set of linear differential equations possesses a general $(N+1) \times (N+1)$ tridiagonal matrix, whose eigenstructure is studied in depth in [9, Sec. A.6.3]. The $N+1$ non-negative, real eigenvalues (and one of them is zero) imply that the eigenvalues c are a discrete set $\{c_0 = 0, c_1, \dots, c_N\}$, so that the Laplace integral in (A17) will reduce to a sum $\varphi(x, t) = \varphi_\infty(x) + \sum_{k=1}^N e^{-c_k t} g(x; c_k)$ for finite size N .

The second-order differential Eq. (A18) in the function g is of the type

$$x^2(1-x) \frac{d^2 g}{dx^2} + (ax+b)(1-x) \frac{dg}{dx} + [\lambda + d(1-x)]g = 0, \tag{A22}$$

where $a = \frac{\varepsilon^*}{\tau} - (N-1)$, $b = \frac{1}{\tau}$, $d = N \frac{\varepsilon^*}{\tau}$, and $\lambda = \frac{c^*}{\tau}$ are real numbers. Unfortunately, (A22) does not seem to be of a known type. Gauss’s hypergeometric function $F(a, b; c; x)$ obeys the differential Eq. [32, Chap. 15]

$$x(1-x) \frac{d^2 g}{dx^2} + [c - (a+b+1)x] \frac{dg}{dx} - abg = 0.$$

Slightly more general, (A18) is of the type

$$p_3(x)g^{(2)}(x) + p_2(x)g^{(1)}(x) + p_1(x)g(x) = 0,$$

where $p_k(x)$ is a polynomial in x of degree k , whereas the hypergeometric differential equation is of the form

$$p_2(x)g^{(2)}(x) + p_1(x)g^{(1)}(x) + p_0(x)g(x) = 0.$$

In conclusion, unless an analytic solution of the differential (A22) can be found, we are afraid that the probability $s_k(t) = \text{Pr}[M(t) = k]$, that the number of infected nodes $M(t)$ at time t equals k in the Markovian continuous-time ε -SIS process on the complete graph K_N , cannot be determined in closed form.

- [1] P. Van Mieghem, Explosive phase transition in SIS epidemics with arbitrary small but non-zero self-infection rate, *Phys. Rev. E* **101**, 032303 (2020).
- [2] A. L. Hill, D. G. Rand, M. A. Nowak, and N. A. Christakis, Emotions as infectious diseases in a large social network: The SISa model, *Proc. R. Soc. B* **277**, 3827 (2010).
- [3] N. A. Christakis and J. H. Fowler, The spread of obesity in a large social network over 32 years, *New England J. Med.* **357**, 370 (2007).
- [4] H. Huang, Z. Yan, and F. Liu, A social contagious model of the obesity epidemic, *Sci. Rep.* **6**, 37961 (2016).
- [5] H. Hinrichsen, Non-equilibrium critical phenomena and phase transitions into absorbing states, *Adv. Phys.* **49**, 815 (2000).
- [6] F. Altarelli, A. Braunstein, L. Dall'Asta, J. R. Wakeling, and R. Zecchina, Containing Epidemic Outbreaks by Message-Passing Techniques, *Phys. Rev. X* **4**, 021024 (2014).
- [7] P. S. Dodds and D. J. Watts, Universal Behavior in a Generalized Model of Contagion, *Phys. Rev. Lett.* **92**, 218701 (2004).
- [8] L. Böttcher, J. Nagler, and H. J. Herrmann, Critical Behaviors in Contagion Dynamics, *Phys. Rev. Lett.* **118**, 088301 (2017).
- [9] P. Van Mieghem, *Performance Analysis of Complex Networks and Systems* (Cambridge University Press, Cambridge, U. K., 2014).
- [10] P. Van Mieghem and E. Cator, Epidemics in networks with nodal self-infections and the epidemic threshold, *Phys. Rev. E* **86**, 016116 (2012).
- [11] C. Li, R. van de Bovenkamp, and P. Van Mieghem, Susceptible-infected-susceptible model: A comparison of N -intertwined and heterogeneous mean-field approximations, *Phys. Rev. E* **86**, 026116 (2012).
- [12] E. Cator and P. Van Mieghem, Susceptible-Infected-Susceptible epidemics on the complete graph and the star graph: Exact analysis, *Phys. Rev. E* **87**, 012811 (2013).
- [13] P. Van Mieghem, Decay towards the overall-healthy state in SIS epidemics on networks, Delft University of Technology, Report No. 20131016, www.nas.ewi.tudelft.nl/people/Piet/TUDELFTReports, arXiv:1310.3980.
- [14] H. Andersson and B. Djehiche, A threshold limit theorem for the stochastic logistic epidemic, *J. Appl. Prob.* **35**, 662 (1998).
- [15] G. Brightwell, T. House, and M. Luczak, Extinction times in the subcritical stochastic SIS logistic epidemic, *Math. Biol.* **77**, 455 (2018).
- [16] P. Van Mieghem and R. van de Bovenkamp, Non-Markovian Infection Spread Dramatically Alters the SIS Epidemic Threshold in Networks, *Phys. Rev. Lett.* **110**, 108701 (2013).
- [17] P. Van Mieghem and R. van de Bovenkamp, Accuracy criterion for the mean-field approximation in SIS epidemics on networks, *Phys. Rev. E* **91**, 032812 (2015).
- [18] P. Van Mieghem, The N -Intertwined SIS epidemic network model, *Computing* **93**, 147 (2011).
- [19] Q. Liu and P. Van Mieghem, Evaluation of an analytic, approximate formula for the time-varying SIS prevalence in different networks, *Phys. A (Amsterdam)* **471**, 325 (2017).
- [20] G. Ferraz de Arruda, F. A. Rodrigues, and Y. Moreno, Fundamentals of spreading processes in single and multilayer complex networks, *Phys. Rep.* **756**, 1 (2018).
- [21] R. Dickman and R. Vidigal, Quasi-stationary distributions for stochastic processes with an absorbing state, *J. Phys. A: Math. Gen.* **35**, 1147 (2002).
- [22] P. Van Mieghem, J. Omic, and R. E. Kooij, Virus spread in networks, *IEEE/ACM Trans. Networking* **17**, 1 (2009).
- [23] P. Van Mieghem, Approximate formula and bounds for the time-varying SIS prevalence in networks, *Phys. Rev. E* **93**, 052312 (2016).
- [24] P. Van Mieghem, SIS epidemics with time-dependent rates describing ageing of information spread and mutation of pathogens, Delft University of Technology, Report No. 20140615, www.nas.ewi.tudelft.nl/people/Piet/TUDELFTReports (unpublished).
- [25] R. Pastor-Satorras and A. Vespignani, Epidemic dynamics and endemic states in complex networks, *Phys. Rev. E* **63**, 066117 (2001).
- [26] J. O. Kephart and S. R. White, Direct-graph epidemiological models of computer viruses, *Proceedings of the 1991 IEEE Computer Society Symposium on Research in Security and Privacy* (IEEE, Piscataway, NJ, 1991), pp. 343–359.
- [27] R. Pastor-Satorras and A. Vespignani, Epidemic Spreading in Scale-Free Networks, *Phys. Rev. Lett.* **86**, 3200 (2001).
- [28] R. Pastor-Satorras, C. Castellano, P. Van Mieghem, and A. Vespignani, Epidemic processes in complex networks, *Rev. Mod. Phys.* **87**, 925 (2015).
- [29] N. T. J. Bailey, *The Mathematical Theory of Infectious Diseases and its Applications*, 2nd ed. (Charlin Griffin, London, 1975).
- [30] D. J. Daley and J. Gani, *Epidemic Modeling: An Introduction* (Cambridge University Press, Cambridge, U. K., 1999).
- [31] P. F. Verhulst, Recherches mathématiques sur la loi d'accroissement de la population, *Nouveaux Mémoires de l'Académie Royale des Sciences et des Belles-Lettres de Bruxelles* **18**, 14 (1845).
- [32] M. Abramowitz and I. A. Stegun, *Handbook of Mathematical Functions* (Dover, New York, 1968).
- [33] E. C. Titchmarsh, *Eigenfunction Expansions Associated with Second-order Differential Equations, Part I*, 2nd ed. (Oxford University Press, London, 1962).